Science of the Total Environment 607–608 (2017) 568–577

Contents lists available at ScienceDirect

Science of the Total Environment

journal homepage: www.elsevier.com/locate/scitotenv

Evaluating the photocatalytic treatment of stevioside by TiO_2 in different aqueous matrices and identification of transformation products

V.A. Sakkas [a], M. Sarro [b], M. Kalaboka [a], V. Santoro [c], T. Albanis [a], P. Calza [b,*], C. Medana [c]

[a] Department of Chemistry, Laboratory of Analytical Chemistry, Ioannnina 45 110, Greece
[b] Department of Chemistry, Via Giuria 5, 10125 Torino, Italy
[c] Department of Molecular Biotechnology and Health Sciences, Via Giuria 5, 10125 Torino, Italy

HIGHLIGHTS

- Photocatalytic transformation of stevioside using titanium dioxide
- The effect of various aqueous matrices and stevioside concentration was assessed.
- A fully nested experimental design was employed.
- More than one hundred unknown transformation products were identified via HPLC-HRMS.
- Assessment of mineralization and acute toxicity using *Vibrio Fischeri* was performed.

GRAPHICAL ABSTRACT

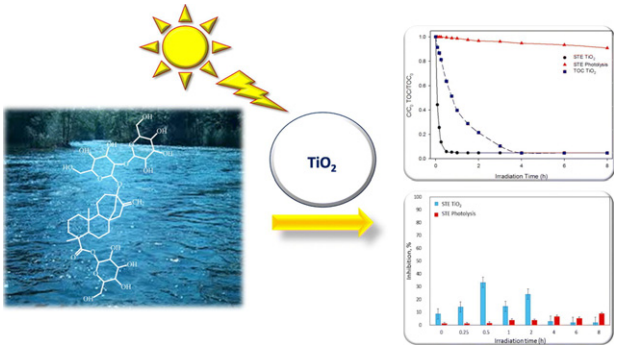

ARTICLE INFO

Article history:
Received 12 May 2017
Received in revised form 30 June 2017
Accepted 2 July 2017
Available online 27 July 2017

Editor: D. Barcelo

Keywords:
Photocatalysis
Stevioside
Sweeteners
Experimental design
Intermediates identification

ABSTRACT

The present study reports the photocatalytic transformation of stevioside, under simulated solar irradiation using TiO_2 as a photocatalyst. As a tool of investigating the effect of various aqueous matrices, as well as, the initial stevioside concentration on the variation of the photocatalytic efficiency, a fully nested experimental design was employed. A significant impact on the degradation rate of the sweetener was observed: degradation rate decreases in the order distilled water > river water > lake water, attributed to the increased natural organic matter content of the respective natural water samples. Moreover, the investigation has involved the identification of intermediate compounds, as well as the assessment of mineralization and toxicity evaluation. More than one hundred unknown transformation products, most of them in the form of several isobaric species, were identified. By employing accurate mass determination, we were able to attribute an empirical formula to each species and through MS^n analyses we were capable to distinguish several isobaric species. The overall transformation mechanism was assessed and involved the hydroxylation/oxidation of the molecule and the subsequent loss of the glucose units bound to the parent compound.

1. Introduction

Artificial and natural sweeteners are widely used in diet soft drinks and foods in order to impart a sweet taste to food and many survive wastewater treatment and have recently been identified as emerging pollutants (Kokotou et al. 2012; Lange et al. 2012; Richardson and Kimura, 2016; Yin et al., 2017). Currently, in the European Union, high-intensity sweeteners (HIS), among them saccharin, sucralose, acesulfame, aspartame, and steviol glycosides are approved as food additives and are mainly used as non-caloric and tooth friendly replacement of sweet-tasting sugars, for obesity treatment, body weight maintenance, management of diabetes etc. (Arbeláez et al. 2015).

* Corresponding author at: Department of Analytical Chemistry, University of Torino, via P. Giuria 5, 10125 Torino, Italy.
E-mail address: paola.calza@unito.it (P. Calza).

http://dx.doi.org/10.1016/j.scitotenv.2017.07.016
0048-9697/

Steviol glycosides, natural sweeteners from the leaves of *Stevia rebaudiana* Bertoni, are ent-kaurene type diterpene glycosides, the most abundant of which are stevioside and rebaudioside A (Wölwer-Rieck et al. 2010).

In principle, sweeteners should be stable in the food matrix both at process and at storage conditions, otherwise, the sweet taste will deteriorate, or there is a possibility that degradation products might give rise to off-flavors in the food products or conduct to possible toxic compounds (Jooken et al. 2012). Recent studies have shown that stevioside is photostable in beverages (Cos et al. 2008), while no sign of decomposition was observed in samples such as milk, yogurt, soy drink, biscuits, jam. On the other hand, Rieck et al. (Wölwer-Rieck et al. 2010) have shown that stevioside was degraded when added to different carbonated soft drinks and stored for up to 72 h at 80 °C. After being discharged from households or excreted mostly unchanged from the human body, the sweeteners flow down the drain and are discharged into the environment through wastewater treatment plants since they are stable under biological, physical and chemical processes (Sang et al. 2014; Subedi and Kannan, 2014). According to our knowledge, the environmental fate and transport of stevioside, as well as physical, biological, and chemical processes that affect its occurrence in natural waters, has not been studied yet. Recently for the first time, a method was developed to determine its occurrence in environmental waters based on SPE and LC-MS/MS (Arbeláez et al. 2015). Nonetheless, stevioside was not detected in any of analyzed samples.

Ecotoxicity of stevioside have already been investigated using tests with green algae *Scenedesmus vacuolatus*, water fleas *Daphnia magna* and duckweed *Lemna minor* (Stolte et al. 2013) but, from our knowledge, no studies have been done on its transformation products. Here, we evaluate the acute toxicity of Steviovide and its transformation products using an acute toxicity test that employs marine bacteria (*Vibrio Fischeri*), particular suitable for the evaluation of ecotoxicity of aquatic systems (Thomas et al. 1999).

Photocatalysis has great potential to be a cost-effective water purification technology for the removal of low concentration recalcitrant organic pollutants, including emerging contaminants such as pharmaceuticals, personal care products, sweeteners etc. (Calza et al. 2010, 2013 and 2017; Sakkas et al. 2007 and 2009).

In the present challenging work, TiO_2 photocatalytic oxidation of stevioside (STE) was investigated for the first time with the scope of determining the degree of variation of the oxidation process under a variety of conditions such as initial stevioside concentration, and water matrix. This approach, especially when chemometric tools are employed – as performed in our study – could identify interactions among the contaminant, the matrix constituent and the photocatalyst, providing more realistic data on the efficiency of the process in natural waters. The latter is of a particular importance since ground and surface waters contain natural organic matter (NOM) such as humic acids as well as various ions, that may interfere with the photocatalytic process (Long et al. 2017; Repousi et al., 2016).

Another objective was the identification of intermediate transformation products since the latter may present a different impact on the environment compared to the parent molecule in terms of toxicity and mobility. For this reason powerful analytical technique such as liquid chromatography (LC) coupled with high-resolution mass spectrometry (HR-MS) was employed.

2. Experimental

2.1. Materials and reagents

Stevioside (1-O-[(5β,8α,9β,10α,13α)-13-{[2-O-(β-D-Glucopyranosyl)-β-D-gluco-pyranosyl]oxy}-18-oxokaur-16-en-18-yl]-β-D-glucopyranose) analytical standard (purity ≥95%), HPLC grade acetonitrile (purity ≥99.9%), and H_3PO_4 (≥99%) were obtained by Sigma-Aldrich (Milan, Italy) and used as received. Experiments were carried out using TiO_2 P25 Evonik (TiO_2) as the photocatalyst. In order to avoid possible interference from ions adsorbed on the photocatalyst, the TiO_2 powder was irradiated and washed with distilled water.

2.2. Photocatalytic degradation experiments

Irradiation experiments of STE took place in a magnetically stirred cylindrical quartz glass UV reactor (inner diameter 6.0 cm, maximum capacity 75 mL). Degradations were performed on 50 mL of aqueous solutions (distilled, river, lake water) at matrix's inherent pH with varying initial STE concentrations (1, 50 and 100 μg/L) at a fixed concentration of TiO_2 (100 mg/L) (Table 1). Before irradiation, the suspensions were allowed to stay in the dark for 45 min under stirring, to reach adsorption equilibrium on the TiO_2. Irradiation was carried out using a Suntest CPS + apparatus from Heraeus (Hanau, Germany) described previously (Calza et al. 2010). The degradation efficiency (expressed as % degradation) was obtained after 15 min of irradiation in the presence of TiO_2.

Experiments on intermediates have been carried out in Pyrex glass cells, filled with 5 mL of STE (20 mg/L) and TiO_2 P25 (200 mg/L). Samples were irradiated for different times (from 5 min to 8 h) with a Philips TLK/05 lamp 40 W with maximum emission wavelength at 360 nm. After irradiation, samples were filtered through a 0.45 μm filter and analyzed with the proper analytical technique.

2.3. Analytical procedures

2.3.1. Measurement of stevioside concentration

After illumination at specific time intervals, samples were withdrawn from the reactor and were filtered through 0.45 μm Millipore disks to remove TiO_2 particles. Quantitative analyses of the residual concentrations of STE were monitored by HPLC apparatus (Dionex Ultimate 3000 Series) consisting of a binary pump with online solvent degasser, an auto sampler with a fixed injection volume of 100 μL, and a DAD-3000 diode array detector. Separations took place on C18 Hypersil Gold Column (250 mm × 4.6 cm; 4.6 μm). All samples were eluted with a linear gradient using 25 mM H_3PO_4 (solvent A) and acetonitrile (solvent B) as the eluent, as follows: 0 min, 30% B; 10 min, 40% B;

Table 1
Design matrix and response data for photocatalytic degradation of stevioside.

Standard order	Run number	A factor: water matrix (type)	B factor: concentration (μg/L)	Response: degradation (%)
1	1	Distilled water	1	85.5
6	2	River water	1	75.5
2	3	Distilled water	1	87.0
10	4	Distilled water	50	80.5
16	5	Lake water	50	52.5
9	6	Lake water	1	60.5
7	7	Lake water	1	58.8
27	8	Lake water	100	46.6
3	9	Distilled water	1	84.1
21	10	Distilled water	100	74.1
11	11	Distilled water	50	78.4
14	12	River water	50	69.2
24	13	River water	100	67.2
4	14	River water	1	76.1
15	15	River water	50	71.2
26	16	Lake water	100	45.6
20	17	Distilled water	100	75.9
25	18	Lake water	100	44.8
12	19	Distilled water	50	76.2
17	20	Lake water	50	51.3
5	21	River water	1	75.1
8	22	Lake water	1	59.7
19	23	Distilled water	100	73.7
23	24	River water	100	64.9
22	25	River water	100	66.1
13	26	River water	50	70.1
18	27	Lake water	50	50.9

20 min, 80% B; and 30 min, 80% B. The flow rate was 1 mL/min and the detection wavelength was selected at 210 nm.

2.3.2. Monitoring of generated transformation products

All samples were analyzed by HPLC/HRMS. The chromatographic separations were achieved with a Phenomenex Luna 150 mm × 2.1 mm, 3 μm, using an Ultimate 3000 HPLC instrument (Thermo Scientific, Milan, Italy). Injection volume was 20 μl and flow rate 0.2 mL/min. A gradient mobile phase composition was adopted: 5/95–95/5 in 45 min acetonitrile/formic acid 0.05% in water. In such condition, retention time for stevioside was 17.26 min. A LTQ Orbitrap mass spectrometer (Thermo Scientific, Bremen, Germany) equipped with an atmospheric pressure interface and an ESI ion source was used. All samples were analyzed in ESI positive mode. The LC column effluent was delivered into the ion source using nitrogen as both sheath and auxiliary gas. The tuning parameters adopted for the ESI source were: capillary voltage 31.00 V, tube lens 135 V. The source voltage was set to 4.5 kV. The heated capillary temperature was maintained at 270 °C. Analyses were run using full mass (50–1000 m/z range with a resolution of 30,000 in FTMS mode. The ions submitted to MS^n acquisition were chosen on the base of full MS spectra abundance without using automatic dependent scan. Collision energy was set to 30 (arbitrary units) for all of the MS^n acquisition methods. MS^n acquisition range was between the values of ion trap cut-off and m/z of the fragmented ion. Xcalibur (Thermo Scientific, Bremen, Germany) software was used both for acquisition and for elaboration.

2.3.3. Total organic carbon analyzer

Total organic carbon (TOC) was measured on filtered suspensions using a Shimadzu TOC-5000 analyzer (catalytic oxidation on Pt at 680 °C). The calibration was performed using standards of potassium phthalate.

2.3.4. Toxicity measurements

The toxicity of samples was evaluated for different irradiation times with a Microtox Model 500 Toxicity Analyzer (Milan, Italy). Acute toxicity was evaluated with a bioluminescence inhibition assay using the marine bacterium *Vibrio fischeri* by monitoring changes in the natural emission of the luminescent bacteria when challenged with toxic compounds. Freeze-dried bacteria, reconstitution solution, diluent (2% NaCl) and an adjustment solution (non-toxic 22% sodium chloride) were obtained from Azur (Milan, Italy). Samples were tested in a medium containing 2% sodium chloride, and the luminescence was recorded after 5, 15 and 30 min of incubation at 15 °C. Inhibition of luminescence, compared with a not-toxic control to give the percentage inhibition, was calculated following the established protocol using the Microtox calculation program.

2.3.5. Experimental design

In order to evaluate the variation of the photocatalytic efficiency (response) of the target molecule, a fully nested experiment consisting of three factors: matrices (distilled water, river water and lake water, $l = 3$), STE initial concentration (1, 50 and 100 μg/L, $p = 3$) as well as replicates ($r = 3$), was conducted. The first source of variability considered was associated with the different nature of the aqueous matrix (and especially the natural organic matter – NOM concentration), being followed by STE concentration (second source of variability) and replicates (last source of variability, considered to have a residual variation). The applied fully nested design consisted of 27 experiments (Table 1). Design-Expert software (trail version 7, Stat-Ease, Inc., MN) was used both for the development of the experimental set-up and for the data analysis.

3. Results and discussion

3.1. Assessment of variation

An obvious obstacle to the performance of the photocatalytic process is the presence of coexisting constituents in the aqueous solutions and especially dissolved natural organic matter (NOM). To evaluate the effect of water matrix, as well as, the initial concentration of the contaminant, used for the preparation of the STE solution, analysis of variance (ANOVA) was performed after the nested experimental design. It should be pointed out that preliminary experiments were carried out, before the development of the experimental design, to evaluate the extent of hydrolysis and photolysis processes on the STE transformation. Results obtained from the adsorption in the dark, hydrolysis as well as direct photolysis showed that the above abiotic processes were scarcely responsible for the observed fast transformations when the solution was irradiated in the presence of the TiO_2.

Considering all effects (Full Model) (Table 2), water matrix, initial STE concentration and their interaction, the Model F-value of 355.37 implies the model is significant since there is only a 0.01% chance that this large value could occur due to noise. Values of Prob > F < 0.0500 indicate model terms that are significant. Our findings indicate that water matrix, initial STE concentration, as well as, their interaction, are significant model terms (Table 2). Moreover, the predicted R^2 value, 0.9858 is in reasonable agreement with the adjusted R^2 value, 0.9909. In light of the diagnostic plots, we can observe from the normal probability plot of the studentized residuals that the data are normally distributed (Fig. 1) indicating a good fit for the model.

From Fig. 2 (interaction effects) we may observe that the photocatalytic efficiency (% degradation after 15 min of irradiation in the presence of titania) varied significantly within each water matrix depending on the initial concentration level of STE. Practically for low initial concentration levels (1 μg/L), the photocatalytic degradation yield was the highest regardless of the composition of the aqueous matrix. As the initial concentration of STE increases (from 1 to 100 μg/L) a decrease of the degradation efficiency is observed for all cases. An increased concentration of the contaminant could occupy more active sites of the catalyst, which inhibits generation of the oxidants, reducing the efficiency of the catalytic reaction (L. Yang et al. 2008). Moreover, intermediate products formed upon the photocatalytic process may compete with the parent molecules for the limited adsorption and catalytic sites on the surface of catalyst particles, and thus inhibit the photocatalytic degradation to a certain extent. Several experimental results indicated that the degradation rates of photocatalytic oxidation of various organic contaminants over illuminated TiO_2 fitted the Langmuir–Hinshelwood kinetics model:

$$-r = \frac{dC}{dt} = \frac{kKC}{1 + KC}$$

where r is the oxidation rate of the reactant, C the concentration of the reactant, t the illumination time, k the reaction rate constant and K is the adsorption coefficient of the reactant. The same kinetic model was

Table 2
Summarized ANOVA for selected nested factorial design.

Source	Sum of Squares	df	Mean Square	F Value	p-value Prob > F	
Model	4078.12	8	502.77	355.37	<0.0001	Significant
A-sources of water	3459.41	2	1729.71	1205.84	<0.0001	Significant
B-Concentration	601.83	2	300.92	209.78	<0.0001	Significant
AB	16.87	4	4.22	2.94	0.0493	Significant
Pure error	25.82	18	1.43			
Cor total	4103.94	26				

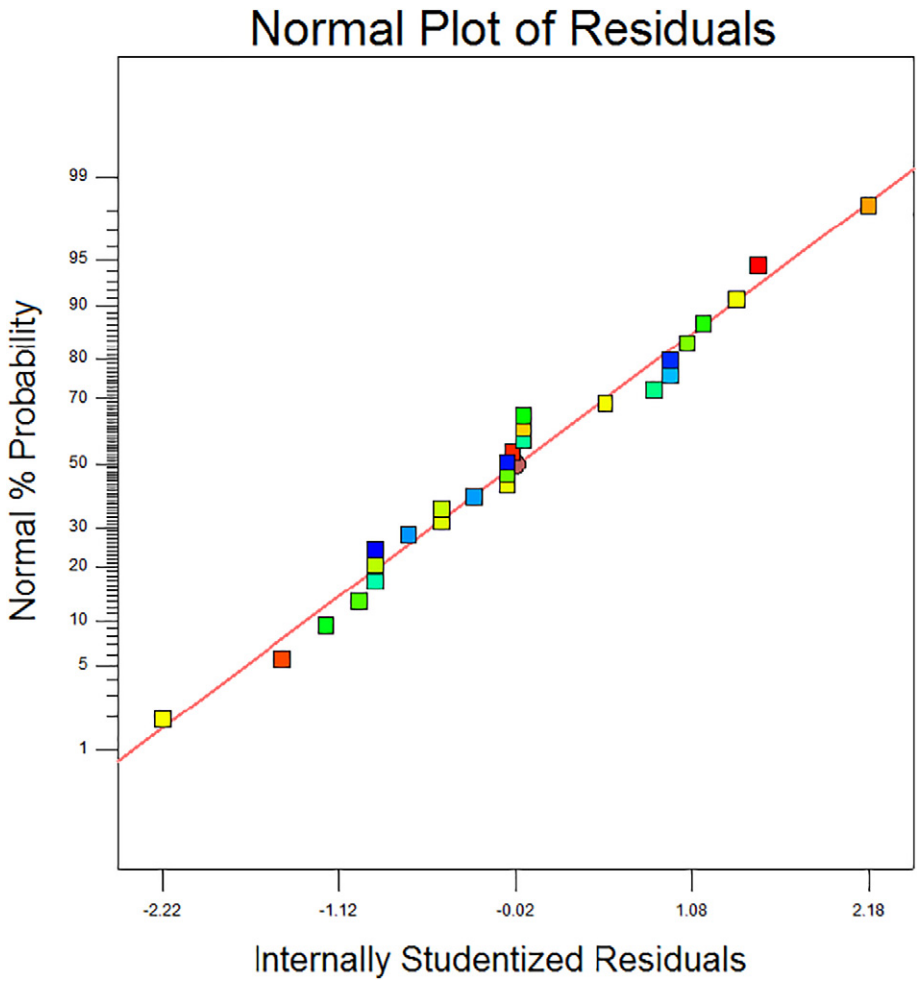

Fig. 1. Residual plots for fitted model.

also confirmed in our study as depicted also by the plots of the natural logarithm of STE concentration versus time (Fig. S1).

The calculated k pseudo-first order rate constants for STE degradation were: distilled water, 0.130, 0.095, 0.063, river water, 0.106, 0.076, 0.049, lake water, 0.088, 0.069, 0.041 min^{-1} for 1, 50 and 100 μg/L, respectively.

In view of the aqueous matrices studied, a significant impact on the degradation rate of the sweetener is observed. The extent of degradation decreases in the order distilled water > river water > lake water. This can be mainly attributed to the increased natural organic matter content of natural water samples (lake water, 12.8 mg/L, river water 2.6 mg/L, distilled water 0.0 mg/L). The inhibition effect of natural organic matter (NOM), which can scavenge photogenerated holes and radicals and prevent reactive oxygen species generation sites upon adsorption is well documented in the literature (Minero et al., 1999; Doll and Frimmel, 2005; Brame et al., 2015) and have been attributed to four mechanisms (Long et al. 2017): i) decrease in contaminant adsorption due to occlusion of active sites on the TiO_2 surface by NOM; ii) decreased generation of reactive oxygen species due to NOM adsorption, iii) direct competition for reactive oxygen species (i.e., scavenging) and iv) radiation attenuation (inner filter effect).

As mentioned earlier adsorption in the dark, hydrolysis and direct photolysis were not responsible for the observed fast transformations of STE when the solution was irradiated in the presence of the TiO_2. Based on these observations we conclude that the inhibition effect in rich NOM waters could be mainly attributed to the competitive reactions with reactive oxygen species and their decreased evolution due to hole scavenging by adsorbed NOM. The possible interference of inorganic ions, which can cause deactivation of the catalyst surface, or the presence of species (e.g. Cl^-, HCO_3^-, CO_3^{2-}) and other reactive moieties competing for OH•radicals (scavengers) should also be considered.

A recent study has shown that phosphate ions counteract the inhibitory effect of humic acids (HA) by decreasing HA adsorption and mitigating electron–hole recombination (Long et al. 2017). Considering that other ions, such as sulfate ions are also ubiquitous in natural waters, it is important to investigate their mechanistic effects and discern how photocatalytic performance is affected by water chemistry (Long et al. 2017). The latter is particular important in order to demonstrate that this technology has the capability to survive outside the laboratory "sterilized" conditions (Cates, 2017).

3.2. Transformation products

STE was irradiated under UV-A alone or in the presence of TiO_2 and analyses were run in HPLC-HRMS, ESI positive mode ($[M + H]^+$ 805.3873). A slight degradation occurred under UV-A and almost 10% of STE was photolysed within 8 h, as shown in Fig. 3.

Along with STE decomposition under UV-A, the formation of 32 transformation products (TPs) occurred and, for most abundant TPs, their evolution profiles are plotted in Fig. 4, while secondary TPs are collected in Fig. S2 in Supplementary information. Most of them were formed from 2 h onward and still persist after 8 h of irradiation.

The addition of the photocatalyst endorsed a fast degradation and STE was efficiently degraded ($t_{1/2}$ 3 min and complete disappearance was observed within 45 min of irradiation). When using TiO_2, even more TPs (118) were detected, whose profiles are plotted in Figs. S3–S11 in supplementary information.

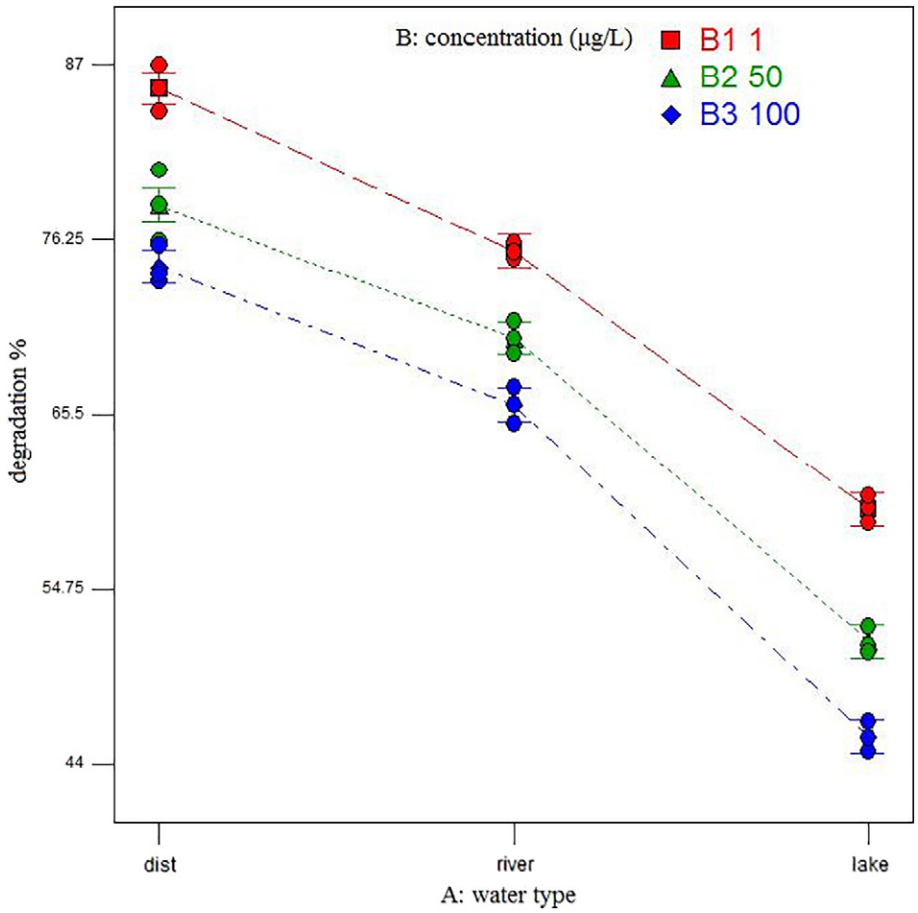

Fig. 2. Scatter plot of actual photocatalytic degradation after 15 min of irradiation in the presence of titania.

Comparing the different evolution profiles over time, it comes up that even if the same kind of TPs are formed through photolysis and photocatalysis, the employment of TiO_2 leads to a higher number of isobaric species. Furthermore, the relative TPs abundance are higher with TiO_2 than via direct photolysis.

During the photocatalytic treatment, the highest TPs level was observed when more than a half of STE was transformed. Most TPs were formed in the initial steps of the photocatalytic treatment and were quickly degraded within 45 min of irradiation, while 4 h of irradiation are required to completely abate them.

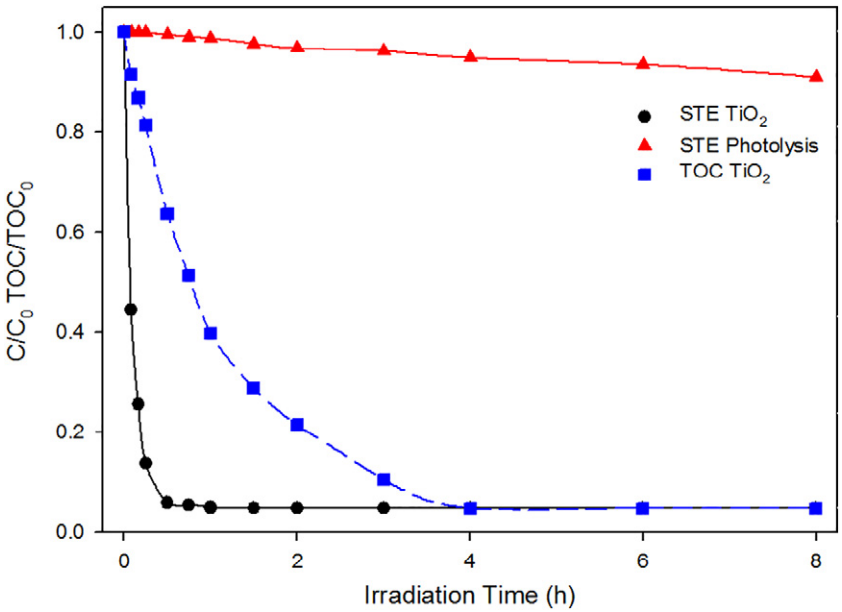

Fig. 3. Stevioside (STE) disappearance under UV-A in MilliQ water alone or in presence of TiO_2 200 mg/L. STE TOC disappearance in the presence of TiO_2 200 mg/L.

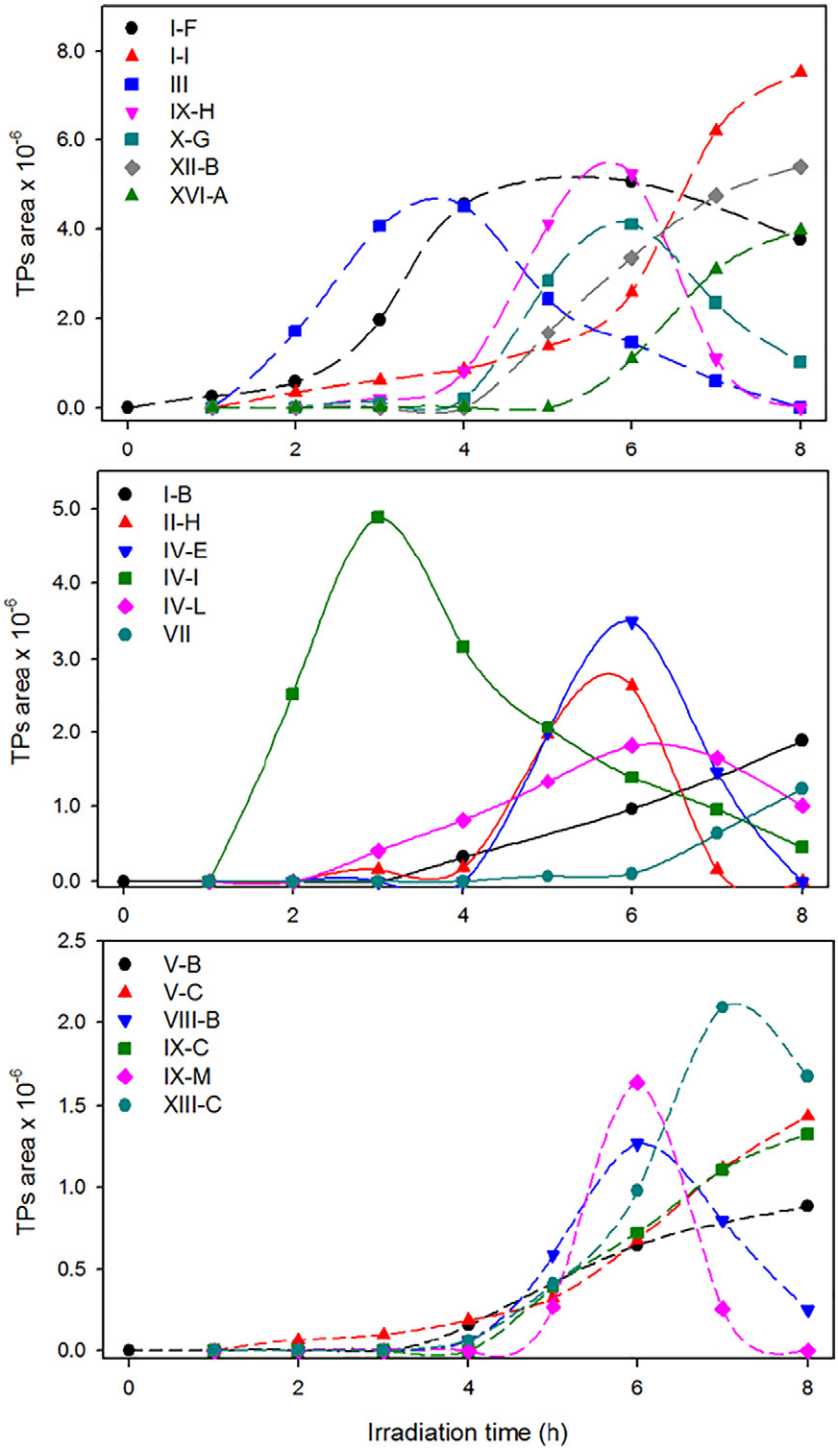

Fig. 4. Transformation products formed from STE under UV-A light.

All TPs are collected in Table 3 and in Scheme 1, while their MS^n product ions are collected in Tables S1–S11 in supplementary information. High resolving power was useful to attribute their empirical formula; accurate *m/z* values of parent ions were reported with error below 1 millimass unit (mmu), which guarantee the correct assignment of their molecular formula in all cases, while their MS^2 and MS^3 spectra showed several structural-diagnostic ions that allowed to characterize the different TPs and to distinguish the isobaric species (see Tables S1–S11). The proposed structures are consistent with MS^2 and MS^3 fragmentation of their protonated forms.

TPs can be grouped into three classes: TPs resulting from (poli)hydroxylation and/or oxidation of the molecule (named **I** to **VI**), those involving detachment of a sugar moiety and a further hydroxylation/oxidation (from **VII** to **XIV**) and finally those resulting from the detachment of two sugar moieties and a further hydroxylation/oxidation (from **XV** to **XVII**).

All TPs belonging to the first group are easily formed. In the presence of TiO_2 they reach the maximum amount within 5–10 min and completely disappeared within 45 min.

Eleven (or three, via photolysis) isobaric species were formed at 821.3825 *m/z* with empirical formula $C_{38}H_{61}O_{19}$ through photocatalytic

Table 3
$[M + H]^+$, name and retention time for all detected TPs: a) TPs formed through photolysis and photocatalytic treatment; b) TPs formed through photolysis only; c) no marks: TPs formed through photocatalytic treatment only.

$[M + H]^+$	Name	t_R (min)	$[M + H]^+$	Name	t_R (min)	$[M + H]^+$	Name	t_R (min)
821.3825	**I-A**	11.67	**851.3543**	**VI-E**	11.54	**673.3419**	**XI-E**[a]	18.86
$C_{38}H_{61}O_{19}$			**$C_{38}H_{59}O_{21}$**			**$C_{33}H_{53}O_{14}$**		
	I-B[a]	12.22		**VI-F**	11.73	**677.3395**	**XII-A**	13.67
	I-C	13.76		**VI-G**	11.85	**$C_{32}H_{53}O_{15}$**	**XII-B**[a]	16.37
				VI-H[a]	12.22		**XII-C**	17.48
	I-D	13.97		**VI-I**	13.73	**693.3343**	**XIII-A**	14.14
	I-E	14.20		**VI-L**	17.06	**$C_{32}H_{53}O_{16}$**	**XIII-B**	14.43
	I-F[a]	14.37		**VI-M**	17.30		**XIII-C**[a]	15.13
	I-G	15.19		**VI-N**[a]	17.39		**XIII-D**[a]	16.37
	I-H	17.39	**643.3334**	**VII**[a]	17.34	**629.3157**	**XIV-A**	11.45
			$C_{32}H_{51}O_{13}$			**$C_{31}H_{49}O_{13}$**		
	I-I[a]	18.12	**641.3178**	**VIII-A**[a]	15.13		**XIV-B**	11.88
	I-L	18.70	**$C_{32}H_{49}O_{13}$**	**VIII-B**[a]	16.37		**XIV-C**	14.18
	I-M	19.65		**VIII-C**[a]	18.12		**XIV-D**	15.50
819.3663	**II-A**	12.83		**VIII-D**	18.70		**XIV-E**	16.39
$C_{38}H_{59}O_{19}$	**II-B**	13.49		**VIII-E**	19.16	**541.2622**	**XV-A**	7.82
	II-C	14.20	**659.3287**	**IX-A**	10.87	**$C_{27}H_{41}O_{11}$**	**XV-B**	8.82
	II-D	14.37	**$C_{32}H_{51}O_{14}$**	**IX-B**	11.67		**XV-C**	9.13
	II-E	14.60		**IX-C**[a]	12.16		**XV-D**	9.32
	II-F	15.01		**IX-D**	12.83		**XV-E**	10.02
	II-G	15.24		**IX-E**	13.91		**XV-F**	10.61
	II-H[a]	18.12		**IX-F**	14.37		**XV-G**[a]	11.32
	II-I	19.77		**IX-G**[a]	15.19		**XV-H**	12.06
817.3510	**III**[a]	17.34		**IX-H**[a]	15.54		**XV-I**	12.55
$C_{38}H_{57}O_{19}$								
837.3740	**IV-A**	10.37		**IX-I**	16.37		**XV-L**	13.22
$C_{38}H_{61}O_{20}$	**IV-B**	12.10		**IX-L**	17.06		**XV-M**[a]	13.58
	IV-C	12.47		**IX-M**[a]	17.34	**495.2595**	**XVI-A**[a]	12.75
	IV-D[a]	12.83	**657.3127**	**X-A**	11.45	**$C_{26}H_{39}O_9$**	**XVI-B**[a]	15.97
	IV-E[a]	13.25	**$C_{32}H_{49}O_{14}$**	**X-B**	11.69		**XVI-C**	18.05
	IV-F	14.37		**X-C**	12.98	**467.2018**	**XVII-A**	8.76
	IV-G	14.60		**X-D**	13.50	**$C_{26}H_{43}O_7$**	**XVII-B**	9.55
	IV-H	15.01		**X-E**	14.54		**XVII-C**	10.08
	IV-I[a]	16.01		**X-F**	15.02		**XVII-D**	10.61
	IV-L[a]	17.34		**X-G**[a]	15.26		**XVII-E**	12.19
	IV-M	18.12		**X-H**	16.21		**XVII-F**	13.76
835.3602	**V-A**	11.67		**X-I**	16.51		**XVII-G**	16.88
$C_{38}H_{59}O_{20}$	**V-B**[a]	13.55		**X-L**	17.14		**XVII-H**	17.40
	V-C[b]	15.13		**X-M**	17.65		**XVII-I**	17.91
	V-D[a]	17.34		**X-N**[a]	18.17		**XVII-L**[a]	18.68
851.3543	**VI-A**	9.76	**673.3419**	**XI-A**	10.99			
$C_{38}H_{59}O_{21}$	**VI -B**	10.20	**$C_{33}H_{53}O_{14}$**	**XI-B**	11.17			
	VI-C	10.87		**XI-C**	11.67			
	VI-D	11.05		**XI-D**[a]	11.92			

or photolytic processes and were attributed to the monohydroxylated STE (namely **I**). For the isomers **I—I**, **I–L** and **I–M**, the formation of a product ion at 319.2273 *m/z*, attributed to the kaurene moiety of the molecule, permits to locate the hydroxyl group on the sugar moieties.

These TPs could then be subjected to oxidation of one (or two) alcoholic groups to keto groups. Nine (or one, via photolysis) TPs with 819.3663 *m/z* were formed and attributed to monohydroxylated/oxidized (namely **II**). A monohydroxylated with a double oxidation was formed as well (817.3510 *m/z*, namely **III**) both under photolysis and photocatalytic treatment.

Eleven (or three via photolysis) compounds at 837.3740 *m/z* were detected and attributed to bi-hydroxylated STE (namely **IV**). In **IVE** and **IV-H**, the formation of a product ion at 333.2067 *m/z* indicates that an oxidation occurred on the kaurene moiety; conversely, the formation of a product ion at 319.2273 *m/z* in **IV-M** suggests that hydroxylation occurred on glucose moieties.

Most of these TPs were further oxidized. Four (or three) bihydroxylated/oxidized were formed at 835.3602 *m/z* (namely **V**) through the photocatalytic or photolytic process, respectively. Twelve (or two, via photolysis) isobaric structures with 851.3543 *m/z* were detected and attributed to trihydroxylated/oxidized derivatives (**VI**).

Lower weight TPs were detected as well and involve the detachment of one (or two) sugar moieties. All these TPs are more slowly formed. During the photocatalytic process they reach the maximum yield within 20–30 min and required longer times (up to 4 h) to completely disappear. Through direct photolysis, they are formed from 5 h onward and persist in the considered time window.

A TP at 643.3334 *m/z* derives from the detachment of a glucose moiety (namely **VII**) and it was formed with both processes; it was further oxidized to form five (or three, via photolysis) TPs with 641.3178 *m/z* (**VIII**). For the isomer **VIII-C** the product ion at 317.2117 *m/z* suggests that the oxidation of an alcoholic group to a keto group occurred in the kaurene moiety of the molecule, while for isomers **VIII-A**, **VIII-B**, **VIII-D** and **VIII-E** the formation of a product ion at 319.2273 *m/z* indicates that the oxidation involved one of the two remaining glucose moieties.

Eleven (or three under photolysis) TPs with 659.3287 *m/z* were formed and attributed to hydroxylation of the deglycosylated molecule (**IX**). The loss of $C_{12}H_{20}O_{11}$, particularly important for **IX-I** to **IX-M**, suggests the detachment of the glucose moiety bond to the ester group. **IX-E** and **IX-F** produces as main product ion 335.2221 *m/z*, thus indicating a hydroxylation in the central part of the molecule. Isomers **IX-H**, **IX-I** and **IX-L** formed the ion at 319.2273 *m/z* as main product ions, suggesting that the transformation does not involve the kaurene moiety of the molecule. **IX** products are further oxidized to produce twelve (or two) TPs with 657.3127 *m/z* (**X**).

Five (or two) TPs at 673.3419 *m/z* are justified by the transesterification of glucose with a methyl group (**XI**). Also in this

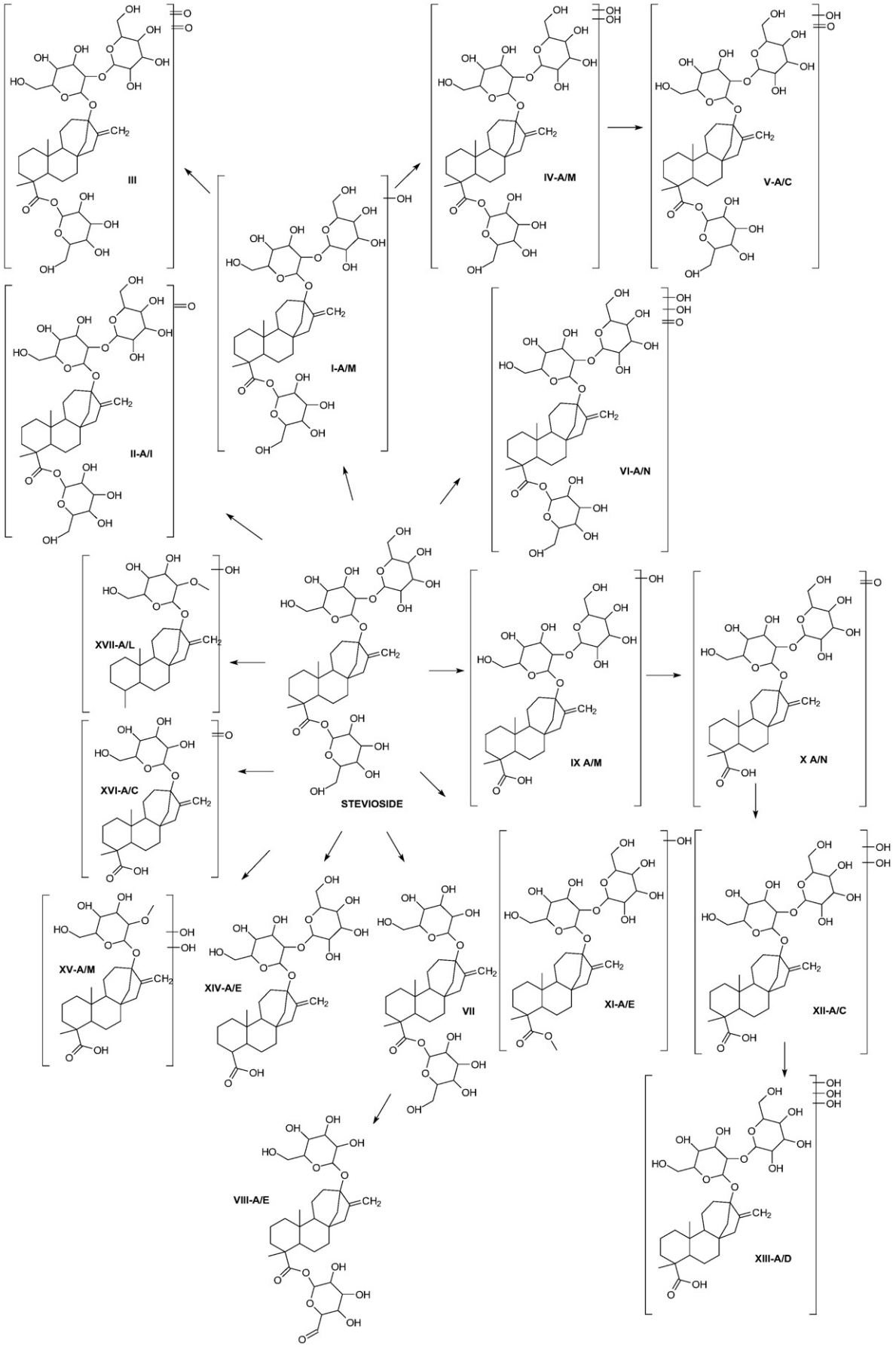

Scheme 1. Proposed transformation pathways followed by STE in the presence of TiO_2 (200 mg/L).

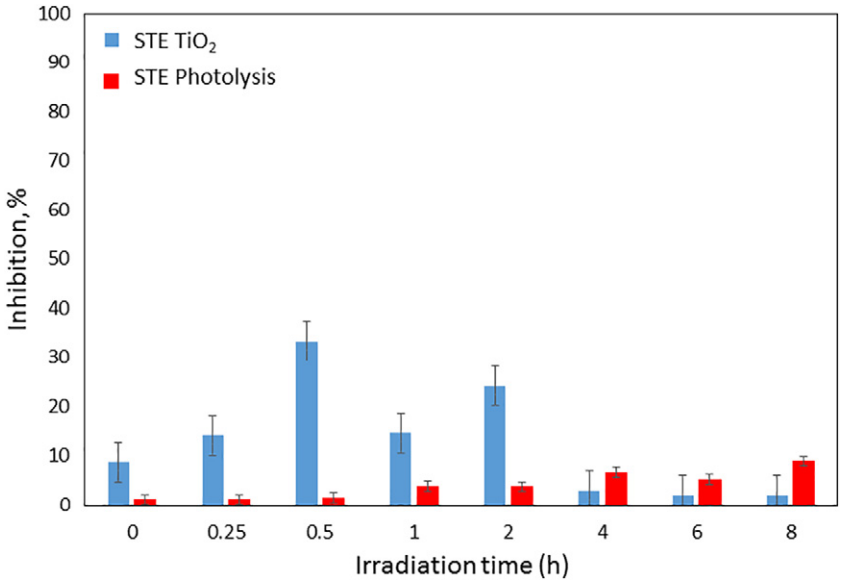

Fig. 5. Acute toxicity of STE as a function of irradiation time through direct photolysis and in the presence of TiO_2. Measures were performed in triplicate.

case, reasonably it has lost the glucose bond to the esther group. For isomers **XI-B** and **XI-C** the methylkaurene ion the methylkaurene ion at 331.1912 *m/z* is formed, while for **XI-D** and **XI-E** the product ion at 333.2072 *m/z* is formed.

Three TPs at 677.3395 *m/z* and four TPs at 693.3343 *m/z* are attributed to bi-hydroxylated and tri-hydroxylated derivatives (namely **XII** and **XIII**), respectively. Five isomers with 629.3157 *m/z* (namely **XIV**) were formed through the photocatalytic process only and their formation involved demethylation from the kaurene moiety and the detachment of a sugar moiety.

The detachment of two molecules of glucose leads to the formation of three TPs, holding 541.2622, 467.2018, 495.2595 *m/z*. The first one involves a dihydroxylation (**XV**) and leads to the formation of eleven (or two) isomers. The second one (**XVI**) presents three isobaric species and involved the hydroxylation/oxidation. The third one (**XVII**) involved the hydroxylation and detachment of the carboxylic group.

3.3. Acute toxicity and mineralization

Acute toxicity was evaluated by monitoring changes in the natural emission of the luminescent bacteria *Vibrio fischeri* when challenged with toxic compounds and was expressed as percentage of inhibition of the bacteria luminescence. Results obtained on samples subjected to photolysis and heterogeneous photocatalysis are plotted in Fig. 5.

STE is not toxic and during the photolysis process, no significant increase in the percentage of inhibition was observed. The toxicity profile during the photocatalytic treatment shows a bell-shaped profile with a maximum at 30 min (inhibition percentage of 30%), thus suggesting the formation of somewhat toxic compounds during the different stages of STE transformation. It has to be underlined that the acute toxicity is insignificant at 4 h of irradiation; at that time, complete STE mineralization was achieved, as assessed by the TOC profile shown in Fig. 3.

4. Conclusions

Our results showed the capability of TiO_2-P25 for the degradation of stevioside in real aqueous samples of different origin, so assessing the photocatalysis as an efficient and environmentally-friendly oxidation process for water treatment. The water composition strongly influences the degradation rate of the sweetener as a decrease in the photocatalytic efficiency takes place in natural waters compared to distilled water. Other than the water matrix, sweetener concentration affected also the reaction efficiency, showing that studying photocatalytic degradation in environmentally relevant conditions is very important. Stevioside was transformed into numerous, slightly toxic, transformation products, all easily degraded.

Acknowledgments

This research has been financed within the European Union's Horizon 2020 research and innovation programme under the Marie Skłodowska-Curie grant agreement No. 645551 (project MAT4TREAT). We acknowledge support by MIUR, in the frame of the collaborative international consortium WATERJPI2013-MOTREM of the "Water Challenges for a Changing World" Joint Programming Initiative (WaterJPI) Pilot Call as well.

Appendix A. Supplementary Data

Supplementary data to this article can be found online at http://dx.doi.org/10.1016/j.scitotenv.2017.07.016.

References

Arbeláez, P., Borrull, F., Pocurull, E., Marcé, R.M., 2015. Determination of high-intensity sweeteners in river water and wastewater by solid-phase extraction and liquid chromatography-tandem mass spectrometry. J. Chromatogr. A 1393:106–614. http://dx.doi.org/10.1016/j.chroma.2015.03.035.

Brame, J., Long, M., Li, Q., Alvarez, P., 2015. Inhibitory effect of natural organic matter or other background constituents on photocatalytic advanced oxidation processes: Mechanistic model development and validation. Water Res. 84, 362–371.

Calza, P., Sakkas, V.A., Medana, C., Islam, M.A., Raso, E., Panagiotou, K., Albanis, T., 2010. Efficiency of TiO_2 photocatalytic degradation of HHCB (1,3,4,6,7,8-hexahydro-4,6,6,7,8,8-hexamethylcyclopenta[α]-2-benzopyran) in natural aqueous solutions by nested experimental design and mechanism of degradation. Appl. Catal. B Environ. 99 (1–2):314–320. http://dx.doi.org/10.1016/j.apcatb.2010.06.038.

Calza, P., Sakkas, V.A., Medana, C., Vlachou, A.D., Dal, Bello, Albanis, F., T. A., 2013. Chemometric assessment and investigation of mechanism involved of photo-Fenton and TiO_2 photocatalytic processes of artificial sweetener sucralose in aqueous media. Appl. Catal. B Environ. 129:71–79. http://dx.doi.org/10.1016/j.apcatb.2012.08.043.

Calza, P., Gionco, C., Giletta, M., Kalaboka, M., Sakkas, V.A., Albanis, T., Paganini, M.C., 2017. Assessment of the abatement of acelsulfame K using cerium doped ZnO as photocatalyst. J. Hazard. Mater. 323:471–477. http://dx.doi.org/10.1016/j.jhazmat.2016.03.093.

Cates, E.L., 2017. Photocatalytic water treatment: so where are we going with this? Environ. Sci. Technol. 51 (2):757–758. http://dx.doi.org/10.1021/acs.est.6b06035.

Cos, J.F., Dubois, D.E., Prakash, I., 2008. Photostability of rebaudioside A and stevioside in beverages. J. Agric. Food Chem. 56:8507–8513. http://dx.doi.org/10.1021/jf801343e.

Doll, T.E., Frimmel, F.H., 2005. Photocatalytic degradation of carbamazepine, clofibric acid and iomeprol with P25 and Hombikat UV100 in the presence of natural organic matter (NOM) and other organic water constituents. Water Res. 39 (2−3), 403–411.

Jooken, E., Amery, R., Struyf, T., Duquenne, B., Geuns, J., Meesschaert, B., 2012. Stability of steviol glycosides in several food matrices. J. Agric. Food Chem. 60 (42): 10606–10612. http://dx.doi.org/10.1021/jf302261j.

Kokotou, M.G., Asimakopoulos, A.G., Thomaidis, N.S., 2012. Artificial sweeteners as emerging pollutants in the environment: analytical methodologies and environmental impact. Anal. Methods 4 (10):3057–3070. http://dx.doi.org/10.1039/C2AY05950A.

Lange, F.T., Scheurer, M., Brauch, H.J., 2012. Artificial sweeteners—a recently recognized class of emerging environmental contaminants: a review. Anal. Bioanal. Chem. 403 (9):2503–2518. http://dx.doi.org/10.1007/s00216-012-5892-z.

Long, M., Brame, J., Qin, F., Bao, J., Li, Q., Alvarez, P.J.J., 2017. Phosphate changes effect of humic acids on TiO_2 photocatalysis: from inhibition to mitigation of electron–hole recombination. Environ. Sci. Technol. 51 (1):514–521. http://dx.doi.org/10.1021/acs.est.6b04845.

Minero, C., Pelizzetti, E., Sega, M., Friberg, S.E., Sjöblom, J., 1999. The role of humic substances in the photocatalytic degradation of water contaminants. J. Dispersion Sci. Technol. 20 (1−2), 643–661.

Repousi, V., Petala, A., Frontistis, Z., Antonopoulou, M., Konstantinou, I., Kondarides, D.I., Mantzavinos, D., 2016. Photocatalytic degradation of bisphenol A over Rh/TiO_2 suspensions in different water matrices. Catal. Today 284:59–66. http://dx.doi.org/10.1016/j.cattod.2016.10.021.

Richardson, S.D., Kimura, S.Y., 2016. Water analysis: emerging contaminants and current issues. Anal. Chem. 88:546–582. http://dx.doi.org/10.1021/acs.analchem.5b04493.

Sakkas, V.A., Calza, P., Medana, C., Villioti, A.E., Baiocchi, C., Pelizzetti, E., Albanis, T., 2007. Heterogeneous photocatalytic degradation of the pharmaceutical agent salbutamol in aqueous titanium dioxide suspensions. Appl. Catal. B Environ. 77:135–144. http://dx.doi.org/10.1016/j.apcatb.2007.07.017.

Sakkas, V.A., Calza, P., Islam, M.A., Medana, C., Baiocchi, C., Panagiotou, K., Albanis, T., 2009. TiO_2/H_2O_2 mediated photocatalytic transformation of UV filter 4-methylbenzylidene camphor (4-MBC) in aqueous phase: statistical optimization and photoproduct analysis. Appl. Catal. B Environ. 90:526–534. http://dx.doi.org/10.1016/j.apcatb.2009.04.013.

Sang, Z., Jiang, Y., Tsoi, Y.K., Sze-Yin Leung, K., 2014. Evaluating the environmental impact of artificial sweeteners: a study of their distributions, photodegradation and toxicities. Water Res. 52:260–274. http://dx.doi.org/10.1016/j.watres.2013.11.002.

Stolte, S., Steudte, S., Helge Schebb, H., Willenberg, I., Stepnowski, P., 2013. Ecotoxicity of artificial sweeteners and stevioside. Environ. Int. 60:123–127. doi.org/10.1016/j.envint.2013.08.010.

Subedi, B., Kannan, K., 2014. Fate of artificial sweeteners in wastewater treatment plants in New York State, U.S.A. Environ. Sci. Technol. 48 (33):13668–13674. http://dx.doi.org/10.1021/es504769c.

Thomas, K.V., Thain, J.E., Waldock, M.J., 1999. Identification of toxic substances in United Kingdom estuaries. Environ. Toxicol. Chem. 18:404–411. http://dx.doi.org/10.1897/1551-5028(1999)018<0401:IOTSIU>2.3.CO;2.

Wölwer-Rieck, U., Tomberg, W., Wawrzun, A., 2010. Investigations on the stability of stevioside and rebaudioside A in soft drinks. J. Agric. Food Chem. 58 (33): 12216–12220. http://dx.doi.org/10.1021/jf102894v.

Yang, L., Yu, L.E., Ray, M.B., 2008. Degradation of paracetamol in aqueous solutions by TiO_2 photocatalysis. Water Res. 42:3480–3488. http://dx.doi.org/10.1016/j.watres.2008.04.023.

Yin, K., Li, F., Wang, Y., He, Q., Deng, Y., Chen, S., Liu, C., 2017. Oxidative transformation of artificial sweetener acesulfame by permanganate: reaction kinetics, transformation products and pathways, and ecotoxicity. J. Hazard. Mat. 330:52–60. http://dx.doi.org/10.1016/j.jhazmat.2017.02.012.